JOURNAL OF MATERIALS SCIENCE **38** (2003) 3933–3944

Effects of chain extender and hard/soft segment content on the surface and electrical properties of PDMS based polyurea-urethane

CHEN-CHI M. MA*, HSU-CHIANG KUAN, JEN-CHIEH HSIEH
Department of Chemical Engineering, National Tsing-Hua University, Hsin-Chu, Taiwan 30043, Republic of China
E-mail: ccma@che.nthu.edu.tw

CHIN-LUNG CHIANG
Department of Industrial Safety and Health, Hung-Kuang University, Sha-Lu, Taiwan 433, Republic of China

A series of PDMS based Poly(urea-urethane) (PUU) polymers with various polar functional groups on their side chains have been prepared by using a prepolymer process. The hydrophilic and hydrophobic characters of PUU films have been investigated. It was found that PUU film possesses different surface properties on the aluminum contacting face and on the air contacting face. Results show that the differences of contact angles between two sides of the PUU film are very significant. Results also indicate that the silicone/nitrogen ratio on the aluminum-contacting surface is higher than that on the air-contacting surface, and the ratio decreases as the hard segment content increased. It was also found that when the sample was in a dry condition, the electrical surface resistance is in the range of 10^{14} Ω. However, when the sample was conditioned at 70%, 80% and 100% R.H., the electrical surface resistance decreases to 10^{8} Ω.

1. Introduction

It is well known that siloxane polymers and elastomers possess some interesting properties such as low density, low T_g, good biocompatibility, good gas permeability, excellent thermal stability, oxidative stability and keep softness and elasticity at low temperature [1]. Due to these advantages, siloxane polymers and elastomers are used widely. The most commonly used siloxane polymer is poly(dimethylsiloxane) (PDMS). PDMS consists of silicone and oxygen atoms and repeats Si—O bonding unit in its backbone chain. The Si—O bond has a high bonding energy and very low bond rotation energy; therefore, PDMS possesses good thermal stability, unusual high flexibility and low T_g [2]. The high flexibility of the Si—O bonding causes PDMS to behave as a viscous liquid above T_g unless it has high molecular weight. The high flexibility also leads PDMS elastomer networks to have weak and poor mechanical properties at room temperature. There are many micro cracks in the elastomer due to the high flexibility of the polymer chain [3]. However, the micro cracks in PDMS elastomers cause it to have high gas permeability.

The methyl groups on the sides of the PDMS backbone chain are very stable and inactive to most functional groups. In addition, the methyl side groups on PDMS possess high hydrophobicity. It also has good oxidative stability and resistance to many chemical reagents. The segment of PDMS within polymers can migrate to the surface to form a hydrophobic surface [4–10]. This hydrophobic and inactive surface possesses low surface energy, hence it can be used in blood contact applications and has anti-thrombogenic character [11, 12], i.e., it has good blood- and biocompatibility.

Polyurea or polyurethane block copolymers exhibit heterogeneous micro phase, where due to the incompatibility of their hard and soft block segments. The soft segment and hard segment in PDMS based Polyurea-urethane are PDMS and diisocyanate, respectively. In this study the mixture consists of 20% 2,4-toluene diisocyanate and 80% 2,6-toluene diisocyanate. There are large differences in structure and properties between soft segment PDMS and hard segment TDI.

The surface composition of copolymer may be determined by X-ray photoelectron spectroscopy (XPS or ESCA). The XPS technique can be used to detect the kinetic energy of photoelectrons, which comes from the inner spherical orbital of elements, and are excited by X-ray. The electrons with same quantum numbers of different elements have different potential energies. This causes excited photoelectrons with different kinetic energies, hence each element has a unique spectrum. From the XPS spectra, one can identify and quantify each element by its peak position and peak area data. The chemical state of elements can be identified

*Author to whom all correspondence should be addressed.

from the information of separated peaks and shifted positions [13, 14].

Another important surface characteristic is hydrophobicity, which can be measured by the contact angle of the PUU film with water. A large tangent angle indicates a higher hydrophobicity. In addition, surface electrical resistance can also be used to describe the behavior of surface hydrophobicity or polarity. The effect of polarity (or hydrophobicity) can be measured from the surface electrical resistance at different relative humidity [15–19].

As many studies have reported that the polysiloxane segments are accumulated on the interface with minimum surface energy, usually on air-contacting surface [20–25]. The effects of siloxane chain length (SCL), molecular weight, casting solvent and annealing temperature on the surface accumulation of siloxane blocks have been discussed [8]. In this study, the PUU copolymer was identified by FT-IR and PUU surface properties were studied by XPS (or ESCA), SEM, water contact angle and surface electrical resistance. The effect of the types of chain extender as well as the effect of the hard segment content on the phase separation and siloxane accumulation of the different surfaces was also investigated.

2. Experimental

2.1. Materials

α,ω-bis(γ-aminopropyl)poly(dimethylsiloxane) ($M_w = 2500$) was purchased from the United Chemical Technologies, Inc., Bristol, PA, U.S.A. Toluene-2,6-diisocyanate (TDI), ethylene glycol, glycerol and 2,2-bis(hydroxymethyl) propanic acid (DMPA) were received from the Lancaster Co. Morecambe, Lancashire, United Kingdom. Stannous octoate (Stannous 2-ethylhexanoate) were obtained from the Sigma Co. Saint Louis, Mo, U.S.A. The PDMS oligomers, glycerol and ethylene glycol were degassed in a vacuum oven at 60°C for 48 h. DMPA was dissolved in the DMF and put in a reaction flask, then degassed at 60°C for 48 h by a vacuum pump. DMF was stirred over MgO for one week, then distilled under vacuum and kept over molecular sieves. THF was degassed by sodium and the distilled before use.

2.2. Synthesis of PDMS based polyurea-urethane copolymers with various chain extenders

The PDMS based polyurea-urethane block copolymers were prepared via the prepolymer process from a diamino-terminated polysiloxane and corresponding diisocyanate and various chain extenders under a nitrogen atmosphere as described in Scheme 1. These reactions were conducted in a 4-neck round bottom flask equipped with a mechanical stirrer, dropping funnel, nitrogen inlet and a condenser. PDMS and TDI were dissolved in THF (1/10 w/v); the two solutions were then mixed and stirred in a reflex at 70°C under a nitrogen atmosphere. FT-IR was used to monitor the N=C=O stretching and C=O stretching of urea at this step. Until the transmittance of NCO stretching peak and CO stretching peak reached a stable ratio (it requires 5 to 7 h), chain extender/THF (1/10 w/v) solution and catalyst stannous octoate were added. FT-IR was used to monitor the N=C=O stretching peak until the NCO stretching peak disappeared, then the solution was kept stirring at room temperature until the viscosity of the solution was observably increased (about 10 h). In these reactions, the $-NCO/(-OH + -NH_2)$ molar ratio is 1.1 and $-OH/-NH_2$ molar ratio is from 0 to 14.

2.3. Preparation of film sample

The polymer was cast on the bottom plate a 70 mm × 70 mm mold with an aluminum foil. The thickness was controlled within 100 μm.

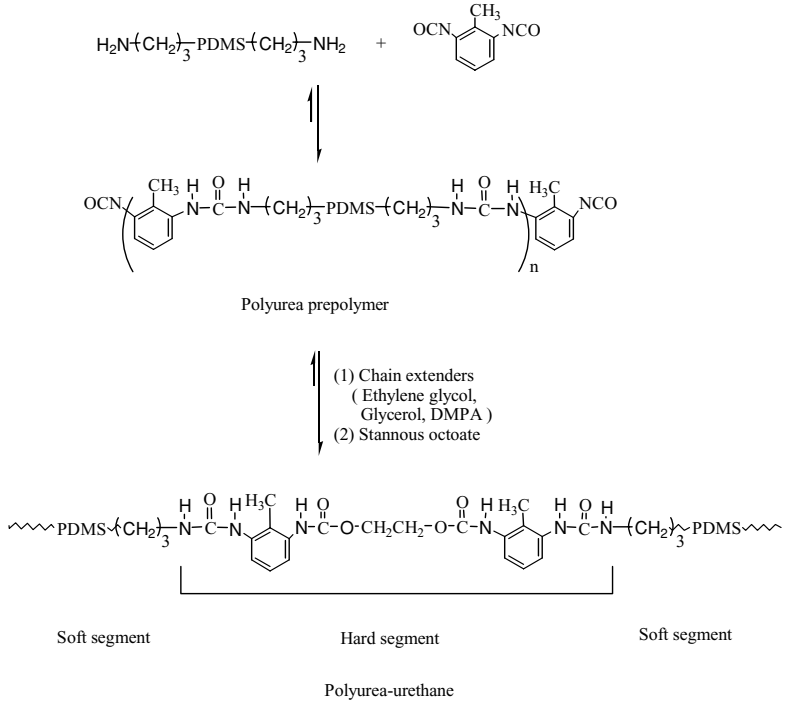

Scheme 1

2.4. Fourier transfer infrared spectroscopy (FT-IR)

FT-IR spectra of the PDMS based PUU were recorded between 400–4000 cm^{-1} on a Nicolet Avatar 320 FT-IR spectrometer, Nicolet Instrument Corporation, Madison, WI., U.S.A. The PUU sample was coated on a KBr plate. A minimum of 32 scans was signal averaged with a resolution of 2 cm^{-1} at the 400–4000 cm^{-1} range. The characteristic absorption peaks of functional group were detected during the synthesis reaction such as N─H stretching at 3500 cm^{-1}, O─H stretching at 3300 cm^{-1}, NCO stretching at 2270 cm^{-1}, C═O stretching of urethane at 1740 cm^{-1}, C═O stretching of urea at 1660 $cm^{-1}$and Si─O asymmetric stretching at 1150 cm^{-1}.

2.5. Contact angle test

The contact angle between the tangent of water droplet and the horizontal plane of the surface of PUU films provides the hydrophobic property measurement. The contact angle was determined on a stable horizontal plane using a goniometer with resolution of $\pm 0.5^{\circ}$. A drop of water with a volume of 1 μL was applied to the surface and the data were recorded within 30 s after the water droplet contacted the PUU surface. An average value was obtained from five to seven measurements for each sample.

2.6. X-ray photoelectron spectroscopy (XPS) or electron spectroscopy for chemical analysis (ESCA)

ESCA or XPS spectra were obtained from a Perkin-Elmer Physical Electronic model 5300 ESCA. Mg K_{α} X-ray source was used under vacuum at 2×10^{-7} torr and 6 kV–30 mA. A take-off angle for the entire sample was 90°. The take-off angle is defined as the direction normal to the surface of the material is 90°.

For quantification of the ESCA signals in carbon 1s, nitrogen 1s, silicon 2p, and oxygen 1s regions, spectra were recorded at high-resolution conditions. ESCA peak areas were measured by a computer with the PHI ESCA version 2.0 software [13].

2.7. Scanning electron microscopy (SEM) analysis

SEM analysis was performed on a JSM-5600 (Japan) model scanning electron microscope with an attached light element detector. Electron beam energy was 15 KV. Data were collected from a scanned region of approximately 100 × 100 square micrometers. The X-ray detector was operated in the thin window mode at less than 20% dead time.

2.8. Electrical surface resistance

The electrical surface resistances of PUU films were measured by megohmeter, which was performed on a Megohmmeter SM-8210 model, TOA Electronic Ltd., Japan. The electrical surface resistances of PUU films were measured after the sample was treated at different relative humidities. The charge time is 20 s and the dc stress of the measurement is 500 V. An average value was obtained from five to seven measurements for each sample.

TABLE I Relationship between the PDMS/Chain extender ratio and the hard segment content of PUU with different chain extenders

PDMS/Chain extender ratio	Hard segment content (weight %)		
	Ethylene glycol	Glycerol	DMPA
1	15.1	15.96	17.05
3	27.57	29.41	31.7
5	36.84	39.15	41.91
7	44.01	46.52	49.47
9	49.72	52.29	55.29
12	56.39	58.96	61.89
14	59.93	62.47	65.23

3. Results and discussion

Table I summarizes the relationship between the PDMS/Chain extender ratios and the hard segment content of PUU with various chain extenders. The hard segments contents in Scheme 1 are calculated by summing the weights of TDI and the chain extender.

3.1. Characterization of PDMS-based polyurea-urethane

Fig. 1 presents the FT-IR spectra of the reaction of PDMS-based polyurea-urethane. The characteristic peak of the N═C═O stretching group of 2,6-toluenediisocyanate (TDI) at 2270 cm^{-1} was detected during the reaction. As the reaction proceeds, the intensity of the NCO group decreased and finally disappeared entirely. The C═O stretching of urea at 1640 cm^{-1} and the C═O stretching of urethane at 1735 cm^{-1} occurred and increased after the second step. As shown in Fig. 1 the chain extender is DMPA, whose ─OH peaks are very broad (3600 cm^{-1}–2600 cm^{-1}).

Figs 2–4 present the FT-IR spectra of different chain extenders with various hard segment contents. As the hard segment content increased, the C═O stretching of the urethane/urea ratio increased. The N─H stretching of urethane differs slightly from that of urea; hence, as the urethane content increased, the N─H stretching groups became broad. No C═O stretching occurred in urethane, however, a sharper N─H stretching peak appeared in Fig. 2, since the associated system did not have a chain extender.

According to Fig. 3, the chain extender is glycerol, and two equivalent of glycerol added as reagent was considered as two equivalent. However, there might be excess hindered by side ─OH group on the left of glycerol molecule. Consequently, the total amount of effective ─OH group is approximately one equivalent. Thus, a broad ─OH stretching peak overlaps the N─H stretching peak, smoothing curve in the region from 3600 cm^{-1}–3200 cm^{-1}.

According to Fig. 4, the chain extender used was DMPA, with one equivalent ─COOH group on the side of it: a very broad O─H stretching peak from 2600 cm^{-1}

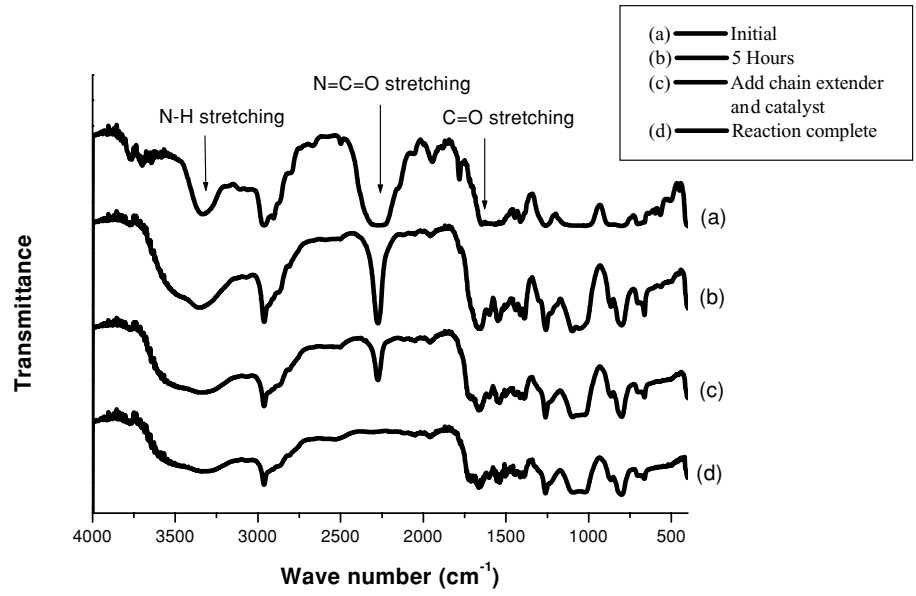

Figure 1 FT-IR spectra of the PDMS based poly(urea-urethane) systems with DMPA as chain extender at various reaction steps.

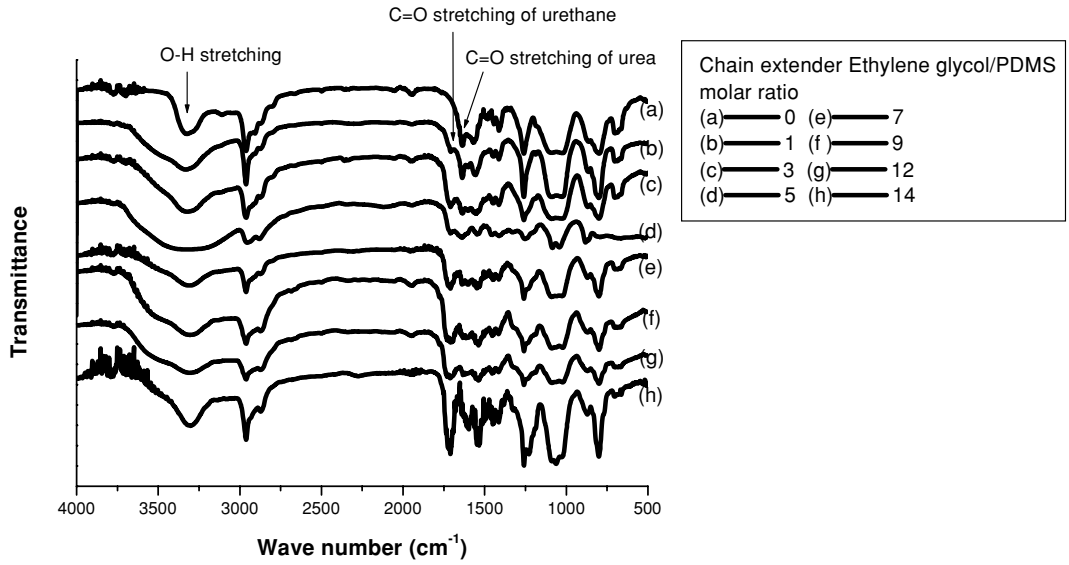

Figure 2 FT-IR stack spectra of PDMS based poly(urea-urethane) systems with ethylene glycol as chain extender and various chain extender/PDMS molar ratios.

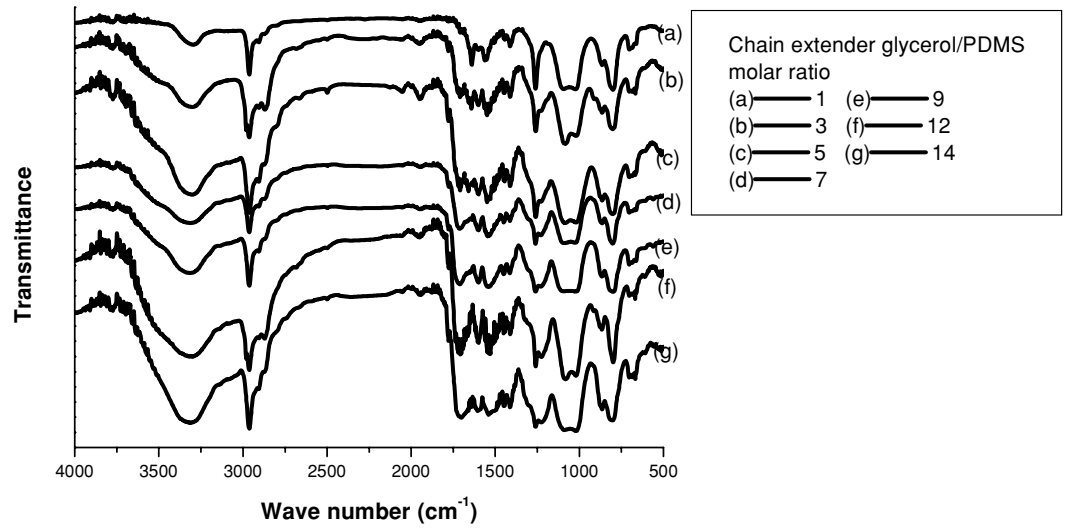

Figure 3 FT-IR stack spectra of PDMS based poly(urea-urethane) systems with glycerol as chain extender and various chain extender/PDMS molar ratios.

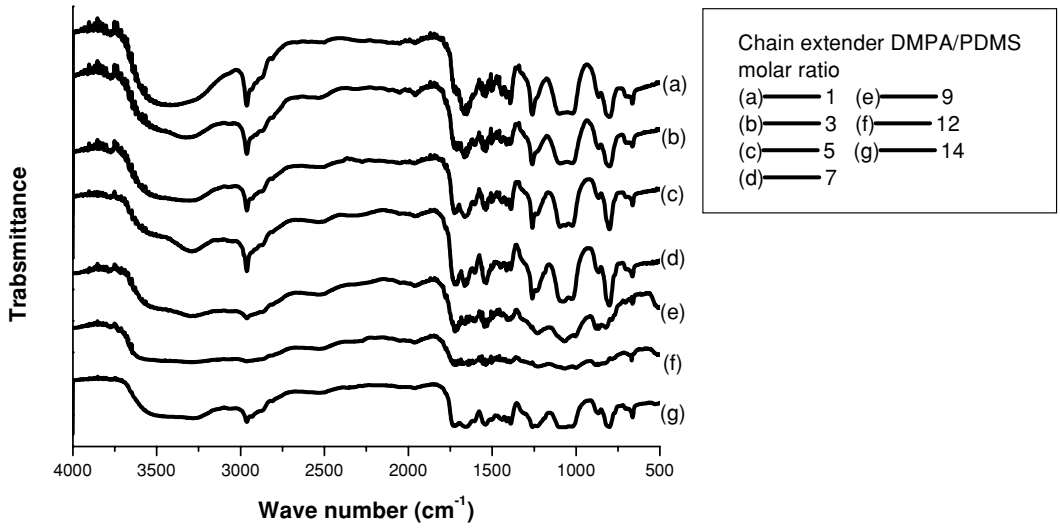

Figure 4 FT-IR stack spectra of PDMS based poly(urea-urethane) systems with DMPA as chain extender and various chain extender/PDMS molar ratios.

to 3600 cm^{-1} was observed. Additionally, the C=O stretching of the −COOH group exceeded and overlapped that of urethane, increasing the breadth and strength of C=O stretching of urethane.

3.2. Effect of chain extender on the XPS

Fig. 5 displays the XPS spectra of the air-contacting surface and the aluminum-contacting surface of PUU with DMPA as a chain extender. According to this figure, the silicon peak on the air-contacting surface exceeds that on the aluminum-contacting surface. The siloxane content and the hard segment content on each side can be compared by measuring the normal areas of nitrogen and silicon element in XPS spectra [8, 15, 26]. The soft segment of PDMS contains only silicon element while hard segments of urea or urethane contain nitrogen element, so the silicon content on the air-contacting side was calculated by measuring the area of silicon element, which exceed that on the aluminum-contacting side. PDMS has a low surface energy, and is stabilized when it migrates to the air-side to form an interface with minimum interface energy [2, 15, 21, 24]. The hard segment content was calculated in the same way and includes significantly more nitrogen on this surface.

Figs 6 and 7 show the XPS stack spectra of air-contacting surface and the aluminum-contacting

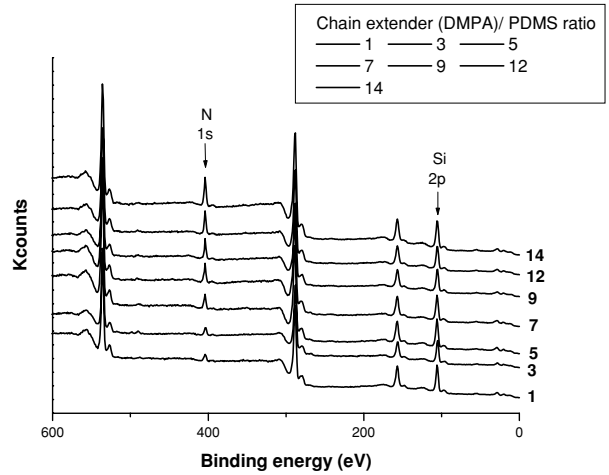

Figure 6 XPS spectra of air-contacting surface of PUU with DMPA as chain extender at different hard segment content.

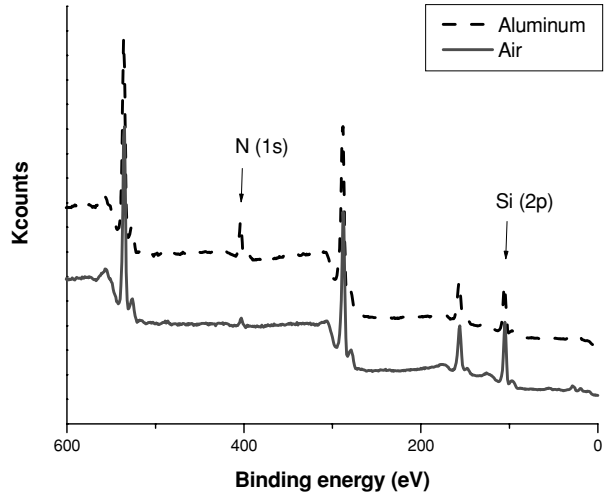

Figure 5 XPS spectra of air-contacting surface and aluminum-contacting surface of PUU with DMPA as chain extender.

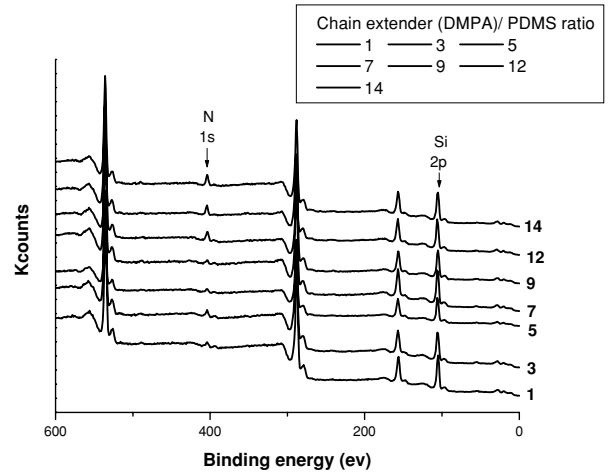

Figure 7 XPS spectra of aluminum-contacting surface of PUU with DMPA as chain extender at different hard segment content.

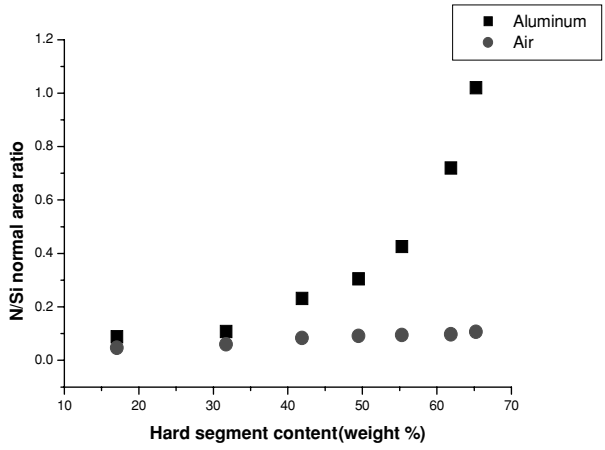

Figure 8 Effect of the hard segment content on the N/Si normal area ratio of PUU with DMPA as chain extender on the air and aluminum-contacting surface.

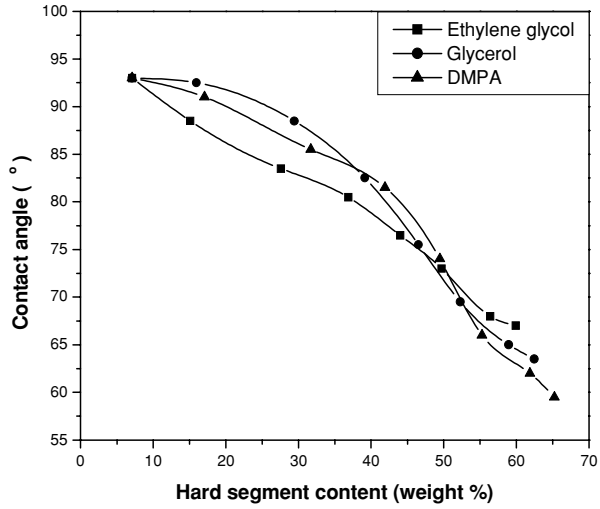

Figure 9 Effects of the hard segment content and the chain extender types on the contact angle of poly(urea-urethane).

surface of PUU with DMPA as the chain extender, with various hard segment contents. As shown in Fig. 6, the nitrogen peaks become larger and the silicone peaks become smaller as the hard segment content in the air-contacting surface is increased. Fig. 7 reveals clear changes of the nitrogen peaks and the silicone peaks of the aluminum-contacting surface. This finding implies that the soft segment and the hard segment content ratios are very similar on the air-contacting side but very different on the aluminum-contacting side. Fig. 8 explicates the N/Si normal area ratio of PUU with DMPA as the chain extender, at the air and at the aluminum-contacting surfaces. As the figure shows, the normal area ratio of nitrogen/silicon (N/Si) of PUU at the aluminum-contacting surface increases with the hard segment content. This observation indicates that the aggregation of the hard segment on this surface increased with the whole hard segment content, reducing the siloxane content on this surface to fall. Furthermore, the N/Si ratios of the air-contacting side are always smaller than those of the aluminum-contacting side. Additionally, the difference between the N/Si of the air and that of the aluminum-contacting side increases with the hard segment content. In relation to that of the aluminum-contacting surface, the change in the N/Si ratio for the air-contacting surface is extremely small and remains almost constant as the hard segment content increases. Specimens of the same thickness closely resemble each other with respect to the siloxane content on the air-contacting surface. However, the siloxane content on the aluminum-contacting surface decreases rapidly as the hard segment content increases, perhaps because the PDMS could almost completely migrate to the lower surface energy side, even if the material has a low PDMS content [2, 7, 8, 15]. This phenomenon is also verified by the measuring hydrophobicity and the water contact angle.

3.3. Effect of chain extender on the contact angle of PDMS based PUU

Fig. 9 plots the hydrophobicity (polarity) of PUU, showing the water contact angle on the aluminum-contacting surface of PUU against hard segment content for different types of chain extender. A greater hard segment content corresponds to a lower water contact angle of the aluminum-contacting surface, and thus, a more polar surface. Furthermore, the type of chain extender is significant. The interactions between water and the functional groups follow the order ionic > polar > nonpolar. In this work, DMPA, glycerol and ethylene glycol were used as chain extenders. DMPA and glycerol contain ─COOH and ─OH polar functional groups side chains, which may increase the amount of polar functional group in the hard segment. The ─COOH group has more lone pairs than the ─OH group. Both functional groups have similar degree of dipole moment, the polarity of the aluminum-contacting surface of PUU, with DMPA as the chain extender, exceeds that of glycerol as a chain extender. Since the ethylene glycol has no polar side group, it should have the lowest polarity on the aluminum-contacting surface. However, the experimental data did not support this expectation. Fig. 9 indicates that PUU with ethylene glycol as a chain extender has the smallest contact angle initially, becomeing the largest finally. This interesting phenomenon might follow from the morphology of the aluminum-contacting surface, which will be elucidated by the SEM microphotographs.

Table II summarizes the water contact angle of pure PDMS and the air-contacting surface of PDMS-based PUU with various chain extenders and different hard segment contents. According to this table, the water contact angles of the air-contacting surface of PUU are all close to those of the pure PDMS and independent of the hard segment content, indicating that the hydrophobicity of surfaces with various hard segment contents closely resembles that of pure PDMS. Fig. 9 also indicates the water contact angle decreases as the hard segment content increases. Furthermore, PDMS is the only hydrophobic segment in the PDMS-based PUU. Hard segment with many lone pair electrons could form more hydrogen bonding with water, reducing its contact angle. This evidence suggest that the

TABLE II Contact angle of pure PDMS and PUU on the air-contacting surface

	Contact angle (°)						
Chain extender/PDMS ratio	0	1	3	5	7	9	12
Chain extender							
DMPA	100.0	99.0	105.0	91.0	98.0	97.0	87.0
Glycerol	114.5	110.0	105.0	98.0	94.0	98.0	95.5
Ethylene glycol	102.0	94.5	107.0	97.0	99.0	96.5	95.5
No chain extender				110			
Pure PDMS				105 ± 2 [16]			

hydrophobic soft segment PDMS will accumulate and be distributed on the air-contacting top surface because of minimum interface energy [15, 16, 17, 27]; while the hard segment content of PUU aggregates on the other surface. This result is consistnet with the XPS spectra, which indicate that the N/Si ratio is much higher on the aluminum-contacting surface and increases with the hard segment content. Additionally, the N/Si ratios remain almost constant on the air-contacting surface, consistent with the similar results in Table II, which reveals that a pure PDMS layer covers the top of the air-contacting surface.

3.4. SEM microphotograph

Fig. 10 displays SEM microphotographs of the air-contacting surface of PUU, with glycerol as the chain extender, for various hard segment contents. The air-contacting surface is almost a homogeneous phase with very few phase-separated spots, regardless of the hard segment contents [7]. This finding follows from the accumulation and covering of PDMS on the air-contacting surface. The PDMS does not aggregate to form a heterogeneous phase-separated surface, but it does form a uniform PDMS-covered layer, which has an amorphous and homogeneous phase, since no hydrogen donor or acceptor is present in the PDMS structure and the Si—O rotation energy is very low.

Figs 11–13 show SEM microphotographs of the aluminum-contacting surface of PUU with various hard segment contents and chain extenders. Comparing to the air-contacting surface, the aluminum-contacting surface is a heterogeneous phase. As the figures show, the samples contain several phase-separated clusters [7, 24]. The number of clusters increases with the hard segment contents, until the clusters finally cover the

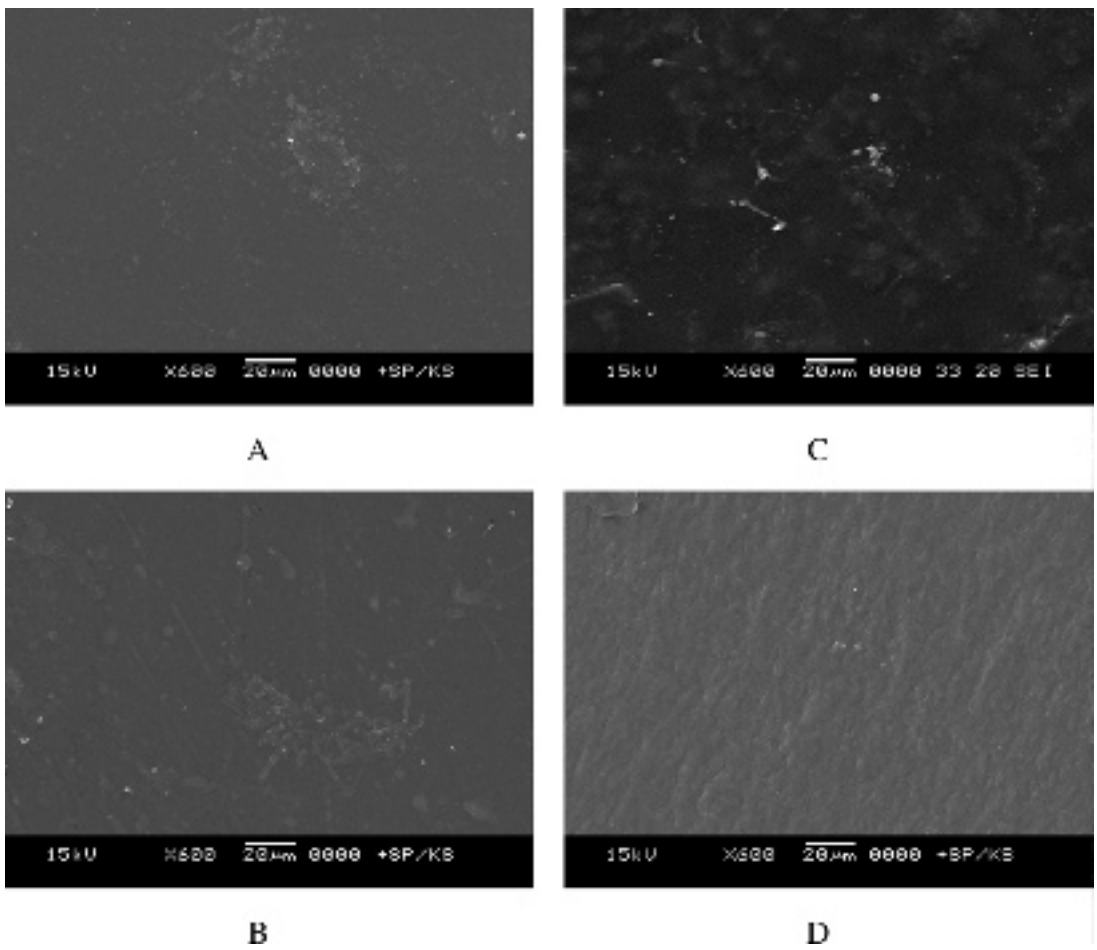

Figure 10 SEM microphotographs of air-contacting surface of PDMS based PUU with glycerol as chain extender. (A) Chain extender/PDMS = 1, (B) Chain extender/PDMS = 5, (C) Chain extender/PDMS = 9, and (D) Chain extender/PDMS = 14.

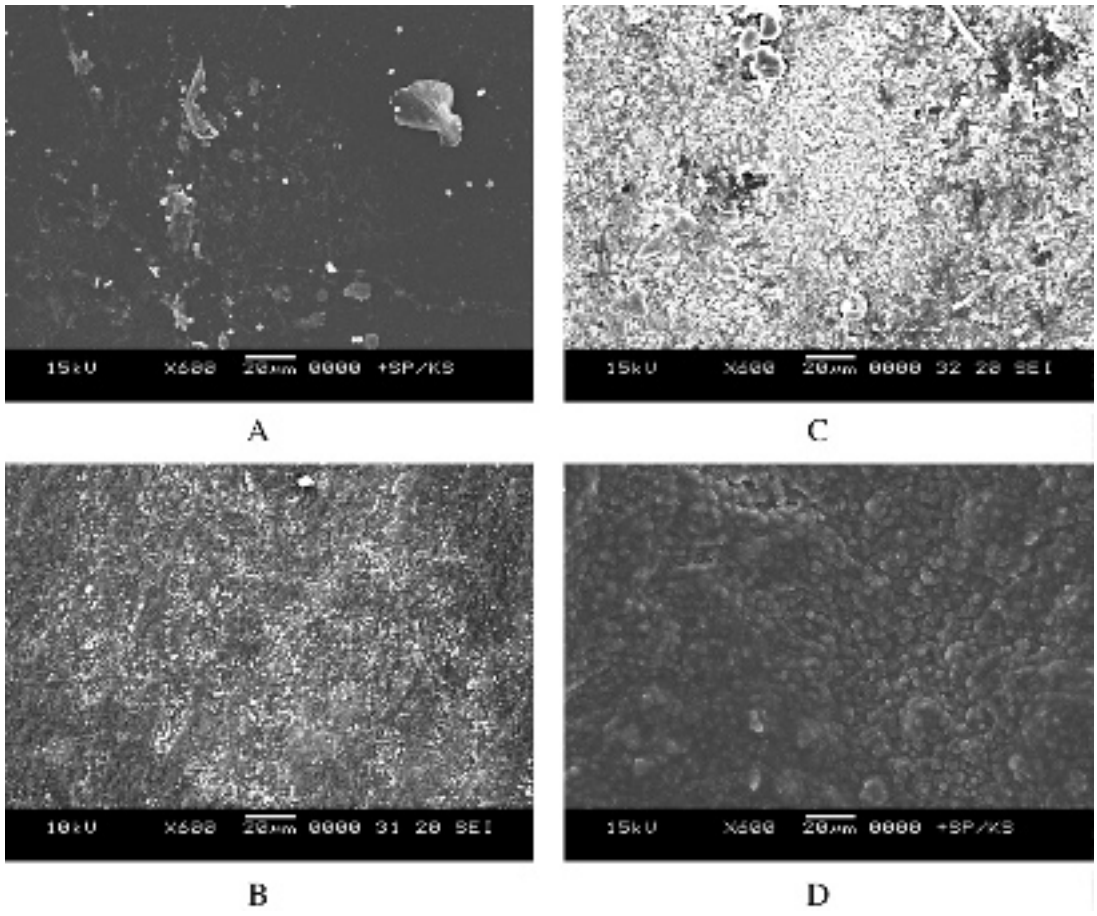

Figure 11 SEM microphotographs of aluminum-contacting surface of PDMS based PUU with glycerol as chain extender. (A) Chain extender/PDMS = 1, (B) Chain extender/PDMS = 5, (C) Chain extender/PDMS = 9, and (D) Chain extender/PDMS = 14.

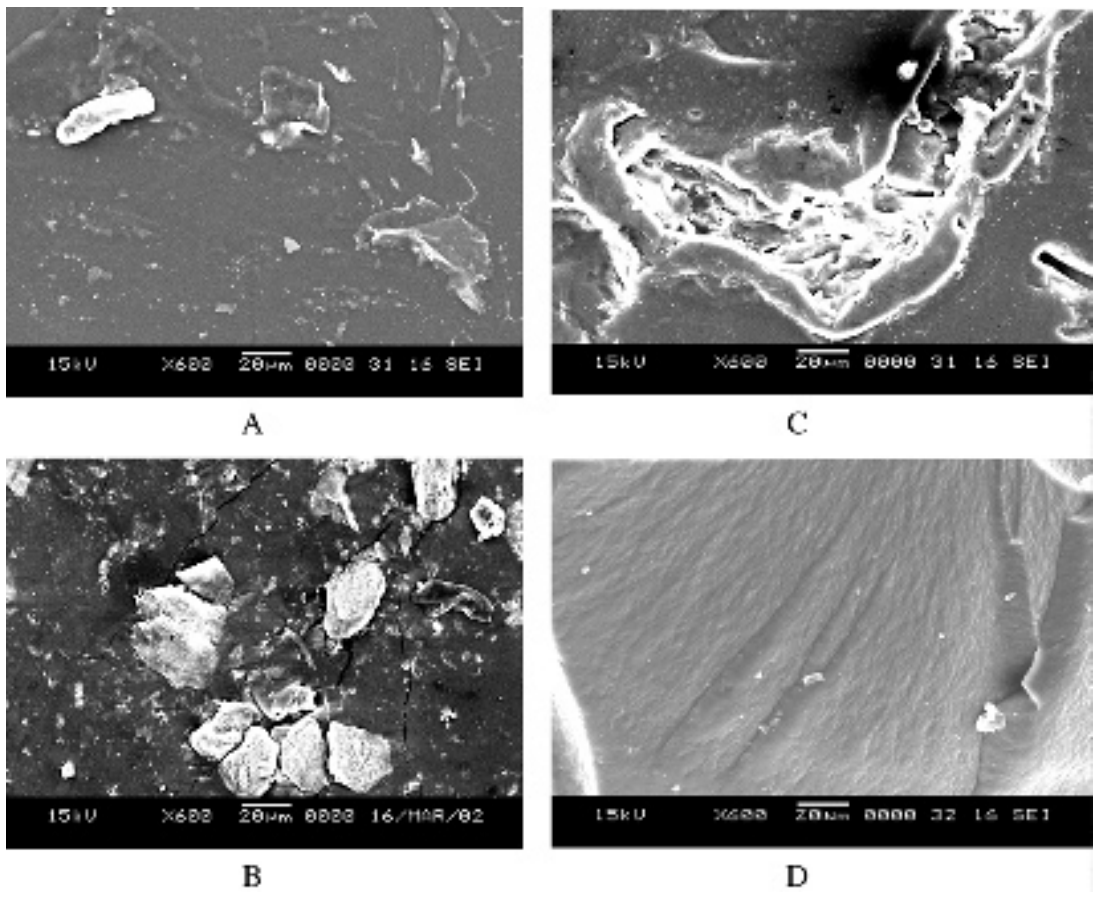

Figure 12 SEM microphotographs of aluminum-contacting surface of PDMS based PUU with DMPA as chain extender. (A) Chain extender/PDMS = 1, (B) Chain extender/PDMS = 5, (C) Chain extender/PDMS = 9, and (D) Chain extender/PDMS = 14.

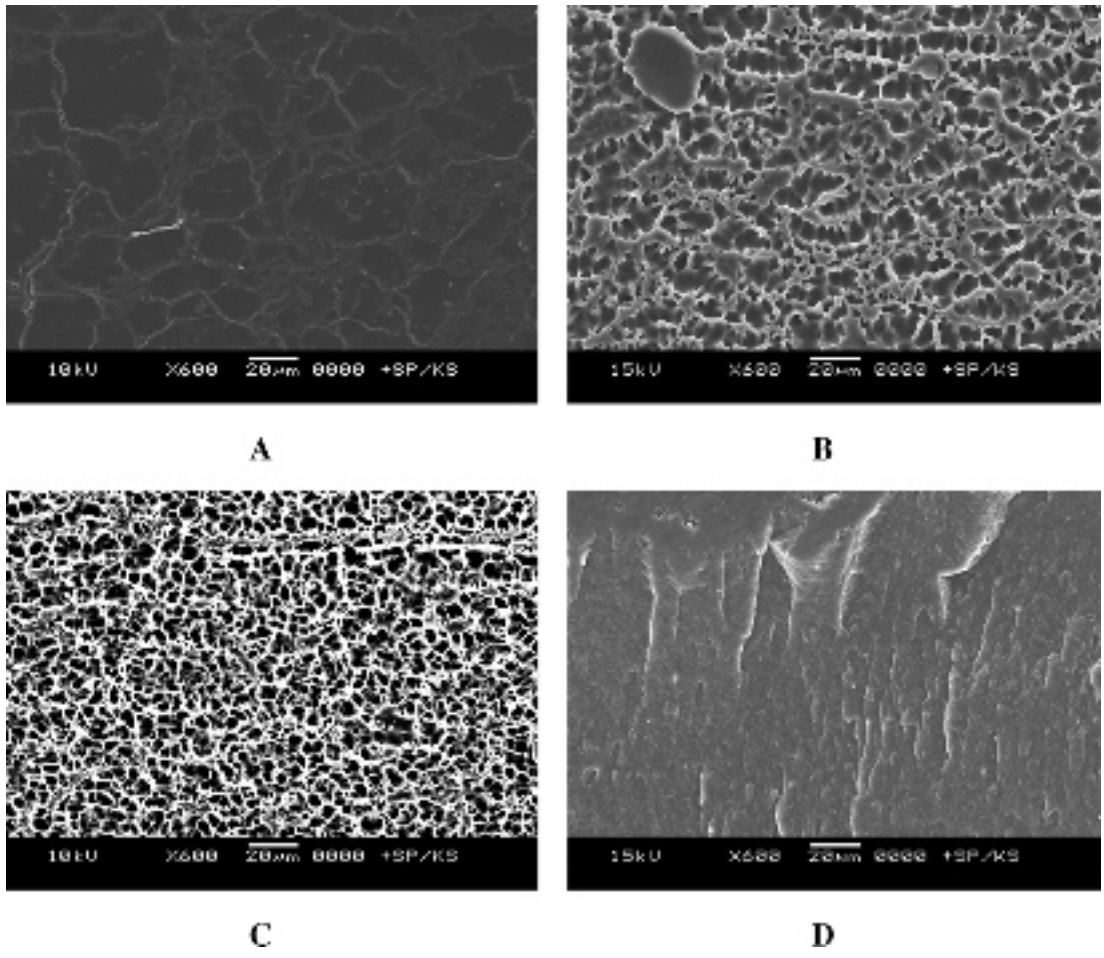

Figure 13 SEM microphotographs of aluminum-contacting surface of PDMS based PUU with ethylene glycol as chain extender. (A) Chain extender/PDMS = 1, (B) Chain extender/PDMS = 5, (C) Chain extender/PDMS = 9, and (D) Chain extender/PDMS = 14.

entire surface of the sample, forming a uniform phase. XPS and the contact angles also indicate a large amount of hard segments on the aluminum-contacting surface. These clusters may, therefore, be formed by the aggregation of hard segments, because they exhibit strong hydrogen bonding.

Different cluster types are generated with different chain extenders. For the glycerol system in Fig. 11, the cluster is a small flake-liked spot, and as the number of the hard segment increasd, the amount of clusters increases, finally forming a heterogeneous surface. For the DMPA system in Fig. 12, the cluster is a large flake-liked spot, and as the hard segment increases, the cluster becomes larger, forming a uniform hard segment, aggregated as a homogeneous surface. For the ethylene glycol system in Fig. 13, the cluster develops a long narrow crack; as the hard segment increases, the cluster becomes wider, finally forming a large cluster. As discussed in the section on the water content angle, the PUU with ethylene glycol as the chain extender has a slightly smaller contact angle as the hard segment content declines. The cluster of the PUU with ethylene glycol as the chain extender is distributed on the surface by narrow strip-like aggregation. However, the PUU with glycerol and DMPA as the chain extenders, form larger aggregated clusters, not distributed like the PUU with ethylene glycol as the chain extender. The reason for these different types of clusters and aggregations is related to the different structures of the chain extenders and the PUU copolymers.

Fig. 14 indicates that PUU with different chain extenders exhibit different types of cluster or aggregation. Different types of cluster follow from the structures of the chain extender and polymers. As mentioned in the experimental section, glycerol and DMPA are considered as two equivalents. Thus, these systems contain fewer active hindered polar side functional groups, ─OH and ─COOH. However, regardless of the hindering of these groups, the side groups ─OH and ─COOH still undergo a few reactions with the ─NCO group, forming T-shape or network-type PUU copolymers. Consequently, clusters of PUU with DMPA or glycerol as the chain extenders have aggregated over a wider area. PUU with ethylene glycol as the chain extender does not form a T-shape structure and so, aggregates less and more narrowly.

The degree of aggregation and the arrangement of the clusters of PUU with DMPA differ from that with glycerol as the chain extender. The aggregation of clusters of PUU with DMPA as the chain extender is more regular. The activation energy of the reaction of ─COOH with ─NCO groups far exceeds that of ─OH and ─NCO [28]. Therefore, the PUU with DMPA as chain the extender may have less of the T-shape structure. The more regular aggregation of the PUU with DMPA as the chain extender follows from the large amount of hydrogen

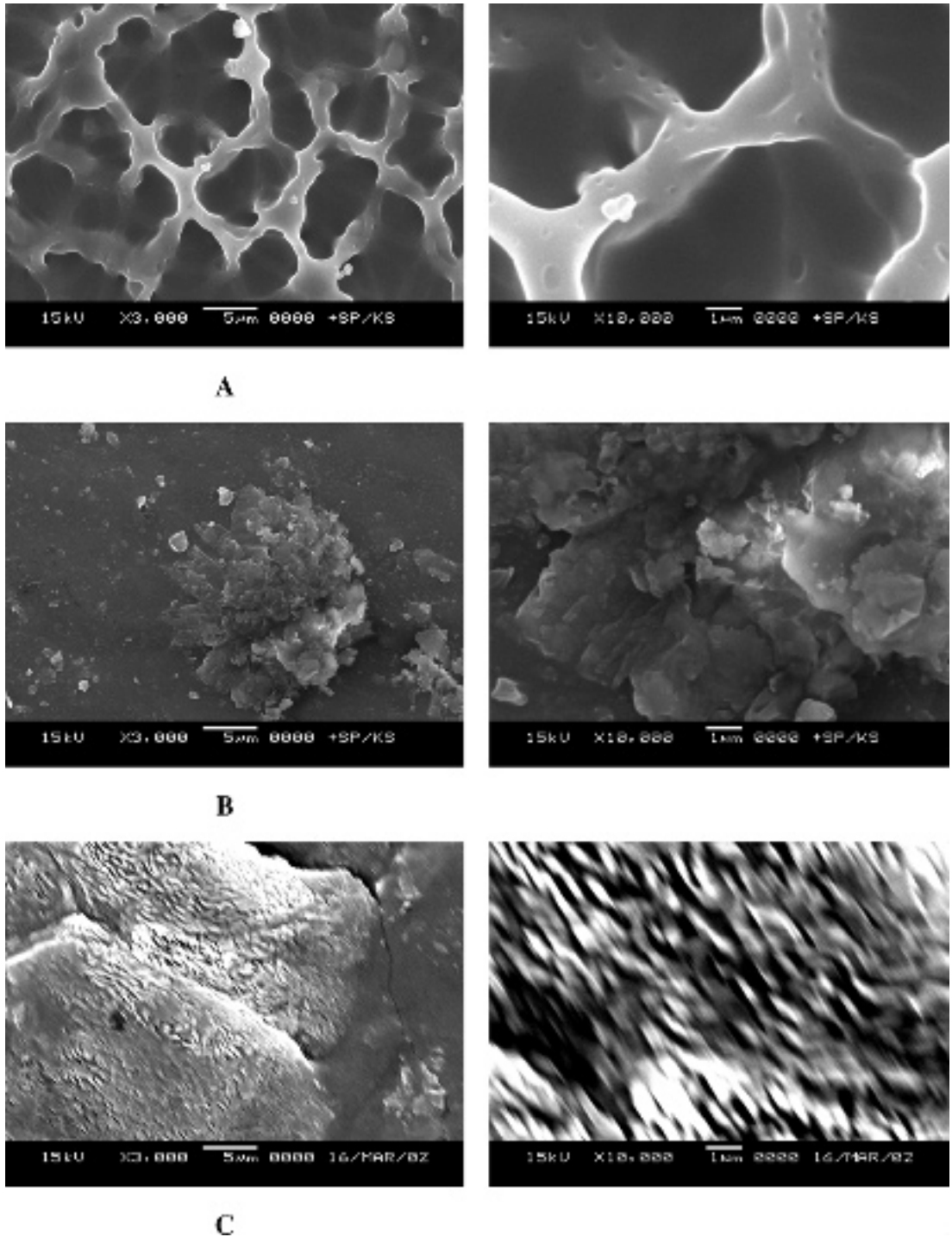

Figure 14 SEM microphotographs of the cluster of PDMS based PUU on the aluminum-contacting surface. (A) Ethylene glycol, (B) Glycerol, and (C) DMPA.

bonding between hard segments. Since the —COOH group is not only a hydrogen donor but also a hydrogen acceptor, it forms hydrogen bonding with another hard segment more easily than the —OH group. Hence, it forms more regular aggregates than PUU with glycerol or DMPA as the chain extender, as shown in Fig. 14B and C.

3.5. Effect of chain extender on the electrical surface resistance of PDMS based PUUs

Fig. 15 plots the relationship between the electrical surface resistance of the aluminum-contacting surface and the hard segment content under dry conditions. It reveals that the electrical surface resistance of PUU exceeds 10^{14} Ω, falling as the hard segment content increases. A greater hard segment content corresponds to more polar functional groups, such that more hard segments accumulate on the aluminum-contacting surface. Therefore, the aluminum-contacting surface becomes more polar and exhibits a more regularly aggregated structure, better able to transfer charge.

Figs 16–18 show that the surface resistance decreased with increasing relative humidity (R.H.). Comparing Figs 15 and 16 reveals that the electrical surface resistances of the sample treated at 70% R.H. is four orders of magnitude lower than that of dried sample.

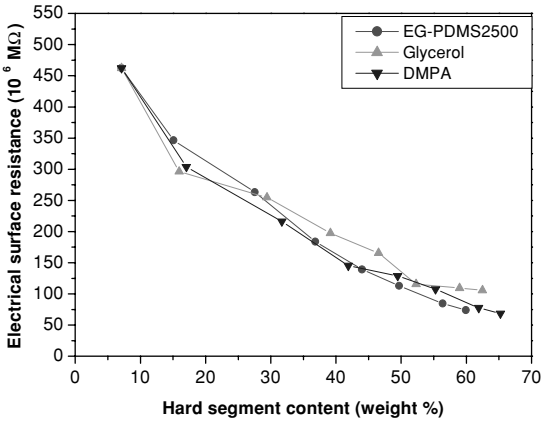

Figure 15 Electrical surface resistance of PDMS based poly(urea-urethane) on the aluminum-contacting surface with various chain extenders and molecular weight of PDMS after dried on the vacuum oven at 80°C for 48 h.

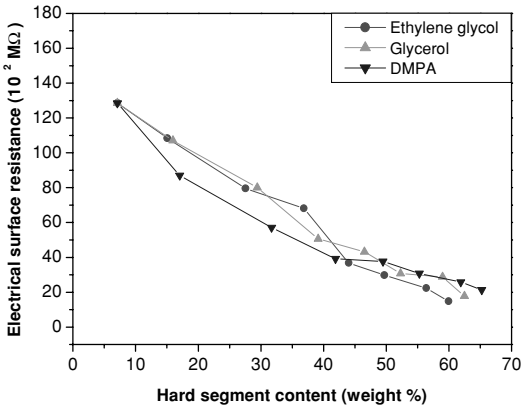

Figure 16 Electrical surface resistance of PDMS based poly(urea-urethane) on the aluminum-contacting surface with various chain extenders and molecular weight of PDMS after treated with 70% relative humidity (R.H.) for 48 h.

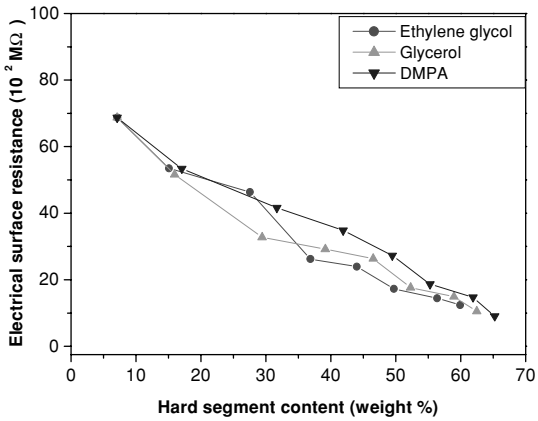

Figure 17 Electrical surface resistance of PDMS based poly(urea-urethane) on the aluminum-contacting surface with various chain extenders and molecular weight of PDMS after treated with 85% relative humidity (R.H.) for 48 h.

Conditioning at 70% R.H. causes the PUU to adsorb water to form a water layer surface, increasing its ability to transfer charge. Furthermore, as the hard segment content increased the electrical surface resistance decreased very rapidly. Fig. 18 illustrates the relationship between the electrical surface resistance and the hard

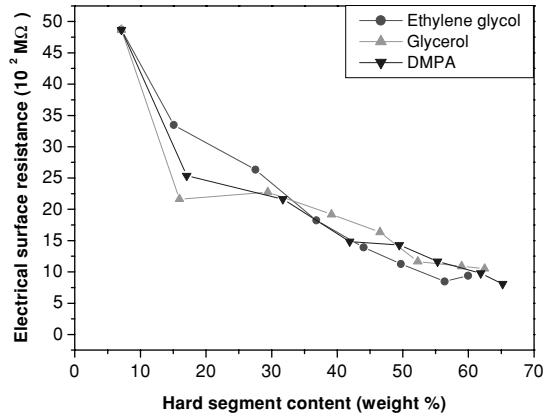

Figure 18 Electrical surface resistance of PDMS based poly(urea-urethane) on the aluminum-contacting surface with various chain extenders and molecular weight of PDMS after treated with 100% relative humidity (R.H.) for 48 h.

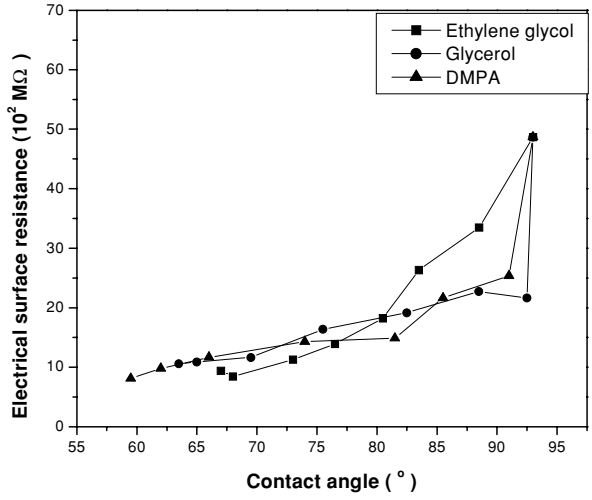

Figure 19 Effect of the contact angle on surface resistance of poly(urea-urethane) after treated with 100% relative humidity (R.H.) for 48 h.

segment content for the sample treated at 100% R.H., the resistance, is generally only one half of that of the sample treated at 70% R.H., implying that a humid environment reduces lower surface resistance, due to water adsorption. The moist material allows the charge to be transferred more easily than in the dried material.

Fig. 19 plots the relationship between the water contact angle and electrical surface resistance for the sample conditioned at 100% R.H. It reveals that at a low contact angle, the electrical surface resistances increases linearly with the contact angle [29]. However, at a high contact angle, the electrical surface resistances for different chain extenders differ at a given contact angle. The electrical surface resistance of PUU with ethylene glycol as the chain extender far exceeds that with DMPA or glycerol as the chain extender at a high contact angle. At a lower hard segment content, DMPA and glycerol, which contain polar functional groups, significantly affect the accumulation of the adsorbed water, reducing electrical surface resistance. However, at high hard segment content, the hard segments of PUU with ethylene glycol as the chain extender may aggregate and form a uniform homogeneous phase on the aluminum-contacting surface, similar to that formed with DMPA

or glycerol as the chain extenders. Therefore, the water-adsorption capacity does not differ significantly among these three types of chain extender.

4. Conclusions

Segregated PDMS-based polyurea-urethane materials were prepared by aminopropyl-terminated PDMS and TDI with different chain extenders. The accumulation of PDMS on the air-contacting surface is proven by XPS, SEM and water contact angle analyses. The results show that the accumulation of PDMS on the air-contacting surface exceeds that on the aluminum-contacting surface. The morphological and topographical information from SEM verifies that the air-contacting surface has a homogenous phase; however, the phase shown on the aluminum-contacting surface is heterogeneous, indicating the presence of a large hard segment content on the aluminum-contacting surface, but only a small content on the air-contacting surface. Surface polarities, derived from the water contact angle, confirm this finding. The hard segment is more polar than the soft segment, so the contact angle of the air-contacting surface exceeds that of the aluminum-contacting surface. Moreover, the contact angles of the air-contacting surface are all close to that of pure PDMS (105°) and the difference between the polarities on the two sides increases with the hard segment content.

Additionally, the type of chain extender influences the aggregation of hard segments. SEM microphotographs present different types of accumulation of hard segments on the aluminum-contacting surface; however, the microphotograph of air-contacting surfaces all show very similar accumulations. The degrees of the aggregation of hard segments on the aluminum-contacting sides are similar for similar hard segment contents. The aggregation of hard segments, randomly dispersed on the aluminum-contacting surface, also suggests that it has a much higher wettability than pure PDMS.

The electrical surface resistance decreased as the hard segment content of PUU increased, or the R.H. declined. The electrical surface resistance was reduced from 5×10^8 MΩ to around 5×10^8 Ω after treatment with 100% R.H. at room temperature.

Acknowledgement

The authors would like to thank the National Science Council of the Republic of China for financially supporting this research under Contract No. NSC 91-2216-E-007-020.

References

1. S. J. CLARSON and J. A. SEMLYEN, "Siloxane Polymers" (PTR Prentice Hall, New Jersey, 1993).
2. W.-Y. CHIANG and W.-J. SHU, *J. Appl. Polym. Sci.* **36** (1988) 1889.
3. C. LI and X. YU, *J. Polym. Sci.: Part B: Polym. Phys.* **26** (1988) 315.
4. G. L. GAINEWS, *Macromolecules* **14** (1981) 208.
5. K.-W. LEE and T. J. McCARTHY, *ibid.* **21** (1988) 3353.
6. T. G. VARGO, D. J. HOOK and J. A. GARDELLA, JR., *J. Polym. Sci.: Part A: Polym. Chem.* **29** (1991) 535.
7. R. BENRASHID and G. L. NELSON, *J. Appl. Polym. Sci.* **49** (1993) 523.
8. X. CHEN and J. A. GARDLELLA, JR. *Macromolecules* **28** (1995) 1635.
9. M. M. GORELOVA and A. J. PERTSIN, *J. Appl. Polym. Sci.* **57** (1995) 227.
10. K. G. MARRA, T. M. CHAPMAN and M. ORBAN, *Macromolecules* **29** (1996) 7553.
11. J. H. SILVER, K. B. LEWIS, B. D. RATHNER and S. L. COOPER, *J. Biomed. Mater. Res.* **29** (1995) 535.
12. A. BRALEY, *J. Macromol. Sci. Chem.* **A4** (1970) 529.
13. G. BEAMSON and D. BRIGGS, Wiley, High Resolution XPS of Organic Polymers: The Scienta ESCA300 Database, 1992.
14. B. V. CRIST, Wiley, Handbook of Monochromatic XPS Spectra, 2000.
15. H. INOUE, A. MATSUMOTO and K. MATSUKAWA, *J. Appl. Polym. Sci.* **41** (1990) 1815.
16. Q. FAN, J. FANG, Q. CHEN and X. YU, *J. Appl. Polym. Sci.* **74** (1999) 2552.
17. M. R. BRUNSTEDT, N. P. ZIATS and M. SCHUBERT, *J. Biomed. Mater. Res.* **27** (1993) 255.
18. I.-K. KANG, D. K. BAEK and YOUNG MOO LEE, *J. Polym. Sci.: Part A: Polym. Chem.* **36** (1998) 2331.
19. J. H. SILVER, K. B. LEWIS, B. D. RATHNER and S. L. COOPER, *J. Biomed. Mater. Res.* **27** (1993) 735.
20. J. ZHAO, S. R. ROJSTACZER and J. CHEN, *Macromolecules* **32** (1999) 455.
21. X. CHEN and J. A. GARAELLA, JR., *Polymer Preprints* (1992) 312.
22. E. L. CHAILOF and E. W. MERRILL, *J. Colloid and Interf. Sci.* **137**(2) (1990).
23. X. CHEN and J. A. GARAELLA, JR., *Macromolecules* **27** (1994) 3363.
24. R. BENRASHID and G. L. NELSON, *J. Polym. Sci.: Part A: Polym. Chem.* **32** (1994) 1847.
25. E. JOHNSTON, S. BULLOCK and J. UILK, *Macromolecules* **32** (1999) 8173.
26. H. INOUE, A. MATSUMOTO and K. MATSUKAWA, *J. Appl. Polym. Sci.* **40** (1990) 1917.
27. S. LIU, L.-T. WENG and C.-M. CHAN, *Surface and Interface Analysis* **29** (2000) 500.
28. J. H. SAUNDERS and K. C. FRISCH, "Polyurethane; Chemistry and Technology," Parts I and II (Interscience, New York, 1962).
29. H. ZHANG and R. HACKAM, *IEEE Trans. on Dielectr. and Electr. Insul.* **6**(1) (1999).

Received 24 December 2002
and accepted 7 July 2003